Efficient photon echoes in optically thick media

M. Azadeh,* C. Sjaarda Cornish,† W. R. Babbitt,‡,‖ and L. Tsang§
Department of Electrical Engineering, University of Washington, Box 352500, Seattle, Washington 98195-2500
(Received 14 July 1997; revised manuscript received 4 February 1998)

We present the results of analytical and numerical calculations of the amplitude and temporal shape of photon echoes produced in optically thick absorbing media. In particular, we are interested in echo output signals that mimic the temporal shape of one of the input pulses (the data pulse). Echo recall efficiencies of temporally structured data pulses exceeding unity can be obtained in optically thick media while preserving the information content of the data pulse. We find that the relationship between the maximum echo efficiency and the Beer's length at which that maximum is attained is nearly linear. This linear relation holds well beyond the optimal absorption length predicted by linear theory for both two-pulse photon echoes and three-pulse stimulated photon echoes. These results have significance in the development of optical coherent transient memory and processing systems, where previous calculations predicted recall efficiencies of only a few percent. [S1050-2947(98)11406-3]

PACS number(s): 42.50.Md, 42.65.−k, 42.25.−p

I. INTRODUCTION

In optical coherent transient systems, information temporally encoded on a data pulse can be stored in an inhomogeneously broadened absorbing medium as a spectral interference grating created by illuminating the medium by a brief reference pulse and the data pulse [1]. The information is recalled by applying a third pulse, resulting in a photon echo signal that mimics the data pulse. Optical coherent transient technology may be employed in a variety of information storage and processing applications with distinct advantages over traditional electronic methods [1–7]. However, a serious hurdle in developing practical coherent transient systems is the relatively low efficiency of the photon echo process [1]. Efficiencies approaching unity are desirable, yet previous studies of echo efficiencies have predicted outputs of only a few percent in absorbing media [8]. While there have been studies on the possibility of improving the efficiency of the echo process by using inverted media [9–12], there is still a wide range of parameter space in absorbing media that is yet to be explored. In this paper, we seek to determine the circumstances under which the maximum echo efficiency can be obtained for weak pulses without distortion of the data pulse structure. Here, recall efficiency is defined as the ratio of the recalled data signal amplitude to the input data signal amplitude. It should be noted that obtaining maximum echo efficiency does not correspond to obtaining maximum signal echo amplitude. In particular, the traditional sequence of pulses with areas $\pi/2$ and π for a two-pulse echo and $\pi/2$, $\pi/2$, and $\pi/2$ for a three-pulse echo—while producing large echo signals—are inefficient (under the above definition) and also lead to distortions of the recall data signals.

In this study we use the standard coupled Maxwell-Bloch equations to predict the data recall efficiency for both two-pulse and three-pulse stimulated photon echoes. We find that efficiencies exceeding unity are achievable under appropriate circumstances. Moreover, under the conditions necessary for high efficiency, the information content of the data pulse is well preserved. The optimum absorption length for maximum efficiency depends on the reference pulses' parameters, and may be on the order of several Beer's lengths. Since this is an inherently nonlinear problem, one must rely on numerical integration of the Maxwell-Bloch equations to determine both the amplitude and shape of the output signals. However, the numerical results for the two-pulse photon echo can be compared to analytical solutions of the area theorem. Although the area theorem does not provide any information about the temporal shape of the pulses, it is still a useful tool for the study of echoes. The information obtained in the two-pulse echo studies can both validate the numerical integration routine used and help in characterizing and understanding the numerically derived results for the stimulated photon echoes.

II. BASIC MODEL

The coherent effect of light on a system of inhomogeneously broadened two-level atoms is governed by Bloch's equations, where the electric field acts as a source for the atomic dipoles. If the pulse propagation effects are to be accounted for, we must also include Maxwell's wave equation, where the atomic dipoles act as a source for the electric field. The coupled Maxwell-Bloch equations govern the coherent lossless interaction of light pulses and atomic dipoles, and are given as [13]

$$\frac{dr_1(z,t,\omega)}{dt} = (\omega-\omega_0)r_2(z,t,\omega), \tag{1}$$

$$\frac{dr_2(z,t,\omega)}{dt} = (\omega_0-\omega)r_1(z,t,\omega)+\Omega(z,t)r_3(z,t,\omega), \tag{2}$$

$$\frac{dr_3(z,t,\omega)}{dt} = -\Omega(z,t)r_2(z,t,\omega), \tag{3}$$

*Electronic address: azadeh@ee.washington.edu
†Electronic address: csc@ee.washington.edu
‡Electronic address: babbitt@physics.montana.edu
§Electronic address: tsang@ee.washington.edu
‖Permanent address: Montana State University, Physics Department, Bozeman, MT 59717.

$$\frac{\partial\Omega(z,t)}{\partial z}+\frac{n}{c}\frac{\partial\Omega(z,t)}{\partial t}=\frac{\alpha}{2\pi}\int_{-\infty}^{\infty}r_2(z,t,\omega)g(\omega), \quad (4)$$

where r_1, r_2, and r_3 are the in-phase, out-of-phase, and inversion components of the polarization, $g(\omega)$ is the inhomogeneous line shape, ω is the transition frequency of the two-level atom, α is the absorption coefficient, n is the index of refraction, and c is the vacuum speed of light. In Eq. (4) it is assumed that the light only propagates in the forward direction, and the laser electric field is assumed to be a plane wave with no phase modulation given by

$$E(z,t)=\frac{\hbar}{\mu}\Omega(z,t)\cos(\omega_0 t-kz). \quad (5)$$

Here ω_0 is the laser carrier frequency, Ω is the electric field in Rabi frequency, and μ is the dipole matrix element of the transition.

III. THE AREA THEOREM

Although the Maxwell-Bloch equations may not be solved analytically in their general form, in the case of the two-pulse photon echo, the validity of their numerical solutions may be checked by comparing the pulse areas calculated from the numerical simulation results to the pulse areas obtained from the analytic solutions to the area theorem. If the area of a pulse is defined as

$$A(z)=\int_{-\infty}^{\infty}\Omega(z,t)dt, \quad (6)$$

then $A(z)$ obeys the following area theorem [15]:

$$\frac{dA(z)}{dz}=-\frac{\alpha}{2}\sin[A(z)]. \quad (7)$$

If $A_1(z)$ and $A_2(z)$ represent the area of the first and second pulses, and $A_e(z)$ represents the total area of all the echoes that are produced as a result of the first two pulses, then using the area theorem one finds that [14]

$$\frac{dA_1(z)}{dz}=-\frac{\alpha}{2}\sin[A_1(z)], \quad (8)$$

$$\frac{dA_2(z)}{dz}=-\frac{\alpha}{2}\cos[A_1(z)]\sin[A_2(z)], \quad (9)$$

$$\frac{dA_e(z)}{dz}=\frac{\alpha}{2}\{\sin[A_1(z)]+\cos[A_1(z)]\sin[A_2(z)]-\sin[A_1(z)+A_2(z)+A_e(z)]\}. \quad (10)$$

Exact analytic solutions to Eqs. (7)–(10) can be calculated as follows. The general solution to the area theorem [Eq. (7)] is, by direct integration,

$$A(z)=2\tan^{-1}\left[\tan\left(\frac{A_0}{2}\right)\exp\left(-\frac{\alpha z}{2}\right)\right], \quad (11)$$

where A_0 is the initial pulse area at the input plane. The solution for Eq. (8), to get A_1, is similar to Eq. (11) and is

$$A_1(z)=2\tan^{-1}[M_1X], \quad (12)$$

where $M_1=\tan(A_{10}/2)$, $X=\exp(-\alpha z/2)$, and A_{10} is the initial pulse area for pulse one. The solution for $A_2(z)$ is obtained by substituting Eq. (12) into Eq. (9), and then integrating to get

$$A_2(z)=2\tan^{-1}\left[\frac{M_2(1+M_1^2)X}{1+M_1^2X^2}\right], \quad (13)$$

where $M_2=\tan(A_{20}/2)$, and A_{20} is the initial pulse area for pulse two. Solving Eq. (10) directly is not trivial, however, recognizing the fact that the sum of all the pulses must also obey the area theorem and thus Eq. (11), their sum can be written as

$$A_1(z)+A_2(z)+A_e(z)=A(z)=2\tan^{-1}\left[\tan\left(\frac{A_{10}+A_{20}}{2}\right)X\right]. \quad (14)$$

The echo area can then be solved for by substituting Eqs. (12) and (13) into Eq. (14), and is

$$A_e(z)=2\tan^{-1}\left[\left(\frac{M_1+M_2}{1-M_1M_2}\right)X\right]-2\tan^{-1}[M_1X]-2\tan^{-1}\left[M_2\frac{(1+M_1^2)X}{1+M_1^2X^2}\right]. \quad (15)$$

The echo pulse area is now expressed simply as a function of z with known parameters for the two input pulse areas, A_{10} and A_{20}. The area theorem equations [Eqs. (8)–(10)] are based on the assumption that all the pulses (including the echo) remain separate from each other in time. In Sec. V, for the cases we studied, we verify the validity of this assumption by numerical methods.

IV. NUMERICAL INTEGRATION OF MAXWELL-BLOCH EQUATIONS

A variety of numerical methods may be used to integrate the set of Eqs. (1)–(4). Specifically, Eq. (4) is the only partial differential equation among the set, and thus may be used as the basis of choosing a solution method. Equation (4) is a

first-order wave equation and has the form of an inhomogeneous advective equation. Therefore, the finite difference method is a suitable way of integrating it. The central difference formula we used has a second-order error, while the usual forward or backward difference formulas have a first-order error.

To carry out the integration we first define a two-dimensional grid. To integrate Eqs. (1)–(3), a third independent variable representing frequency has to be defined as well. This variable models the inhomogeneous broadening that is responsible for the production of the photon echoes. The inhomogeneous bandwidth of the medium determines the shortest pulse that may propagate in the medium without distortion. In our simulations, we chose an inhomogeneous bandwidth that was sufficiently greater than the bandwidth of our data so as not to cause distortions in the echo. Increasing the inhomogeneous bandwidth had little effect on our results. Decreasing the inhomogeneous bandwidth, to first order, would reduce the efficiency of the echo similar to a low-pass filter.

The initial conditions of the problem are the states of the dipoles in the medium at $t=0$. All the dipoles are initially assumed to be in the ground state ($r_1=r_2=0$, $r_3=-1$). This condition corresponds to the case of an absorbing medium. The variables r_1, r_2, and r_3 can also be altered after each pulse to simulate coherence loss, population decay, or population transfer.

V. TWO-PULSE PHOTON ECHO

We must first check the validity of the numerical solutions of Eqs. (1)–(4) by comparing the area of the echo pulse to that predicted by the area theorem. In the numerical simulations, we consider the case of a data pulse followed by a brief pulse, which causes the sample to reemit a time-reversed replica of the data pulse.

In this study by *data pulse* we mean a weak pulse that has a known temporal structure and information content. We have purposely chosen a weak data pulse (well within the linear response regime). In a practical system the data sequence may consist of thousands of subpulses. In order not to saturate the absorbing material, the subpulses must be very weak, so that their combined area does not cause distortion in, or reduce the efficiency of, the recalled wave form. Finally, there are many optical processing applications in which one would choose to operate coherent transient devices in the linear (unsaturated) regime. In practice, once the conditions for maximum efficiency are found, the input data pulse's amplitude could be increased to just below the point of saturation to maximize the output amplitude to the point where the efficiency is only slightly sacrificed and the output signal is only slightly distorted. However, we chose to operate well within the linear regime for the data pulse, where the output signal is directly proportional to the echo signal amplitude (i.e., minimal pulse broadening), so that the recall efficiency is independent of input data amplitudes.

A *brief pulse* is considered to be a pulse much shorter than the shortest time structure in the data pulse, or equivalently, with a Fourier-transform-limited bandwidth much larger than the data pulse. In our numerical simulations the brief pulse is intentionally chosen to be three times shorter than each of the subpulses in the data pulse. In this way, the brief pulse acts more or less as a delta pulse with respect to the data, and thus convolution distortions are minimized [16]. From a mathematical point of view the brief pulse should be chosen to be much shorter than each of the subpulses, but memory and computational power constraints limit the shortest possible brief pulses in the numerical simulation. Interestingly, in practice, similar limitations exist due to constraints on the laser power, which limit the shortest possible obtainable pulse with a certain pulse area. The timing between the data pulse and the brief pulse is not critical as long as the pulse separation is short compared to the homogeneous decay time of the material.

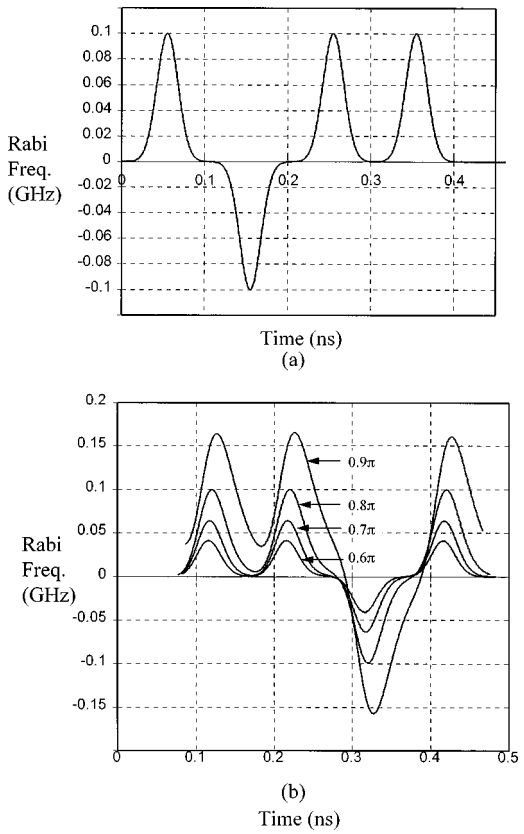

FIG. 1. (a) Input data pulse, (b) two-pulse echo outputs for values of the brief pulse varying from 0.6π to 0.9π. The amplitudes are given in Rabi frequency.

To verify the assumption in the area theorem that the pulses indeed remain separate in time, we must look at the temporal envelope of the input data and the echo pulse as they propagate through the absorbing medium. The full numerical integration of the set of Eqs. (1)–(4) contains this information, and more importantly, it predicts the shape of the echo pulse. In practical applications of coherent transients it is necessary to consider distortion, or fidelity of the output signal with respect to the input data. The determination of the conditions under which one obtains maximally efficient echoes while preserving information content is the primary objective of the numerical simulations.

Figure 1 shows the actual pulse shape of the input data and the pulse shape of the echo signal (calculated at an αz where the echo signal is maximum) predicted by a full numerical integration of Eqs. (1)–(4). The amplitude of the data pulse is 100 MHz (Rabi frequency), and the data pulse

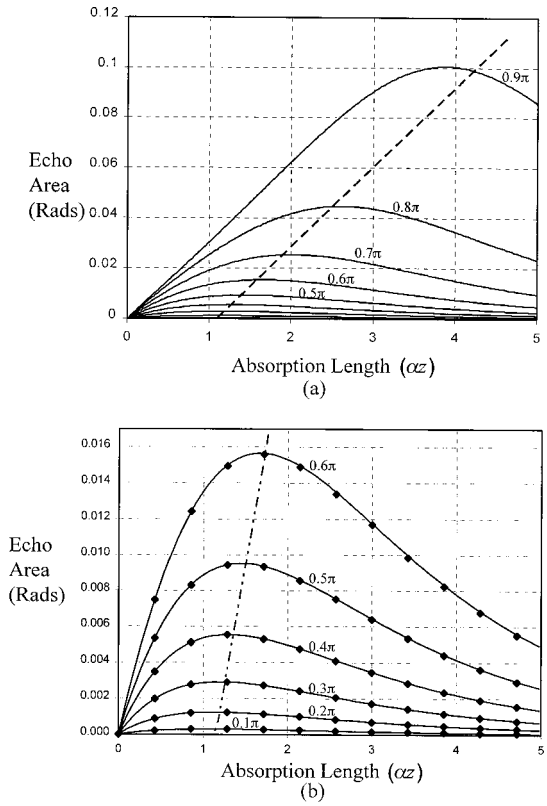

FIG. 2. Two-pulse photon echo area for a data pulse of 0.01π and brief pulse areas ranging from 0.1π to 0.9π calculated using the area theorem. The linear fit to the maximum points is also shown (dashed line). Case (b) is the zoomed version of case (a), along with the predicted area (diamonds) using the numerical simulations of the Maxwell-Bloch equations.

itself is an asymmetric combination of four Gaussian subpulses each 0.09 ns long, and 0.01 ns apart from each other [Fig. 1(a)]. The area of each of these subpulses is 0.005π. This choice of data pulse structure (compared to a single pulse) allows for a better study of distortion effects and the degree to which the output echo signal retains the information content of the input data pulse as it propagates in the medium. The choice of the data pulse sequence $\{1,-1,1,1\}$ allows us to study the intersymbol interference between adjacent in-phase and out-of-phase subpulses. The brief pulses used were Gaussian pulses 0.03 ns long.

When using the area theorem, only the area of the data and brief pulse is of consequence. Unlike the numerical simulations, the area theorem does not provide a means through which temporal modulation of the data pulse can be studied. The data pulse is defined simply as an area, and in this case it is set equal to the total area of the data pulse used in the numerical simulations, thus $A_{10}=0.01\pi$. We use Eqs. (12), (13), and (15) to predict the evolution of the area of the first two pulses as well as the echo pulse.

Figure 2 shows the area of the echo as a function of absorption length (αz) for a constant data pulse area of 0.01π and different brief pulse areas ranging from 0.1π to 0.9π. In Fig. 2(b) we have also plotted the echo area calculated from the data obtained by the numerical integration of the coupled Maxwell-Bloch equations. The Maxwell-Bloch simulations and the area theorem predict nearly identical results. One can also see that the maximum echo area increases when the area

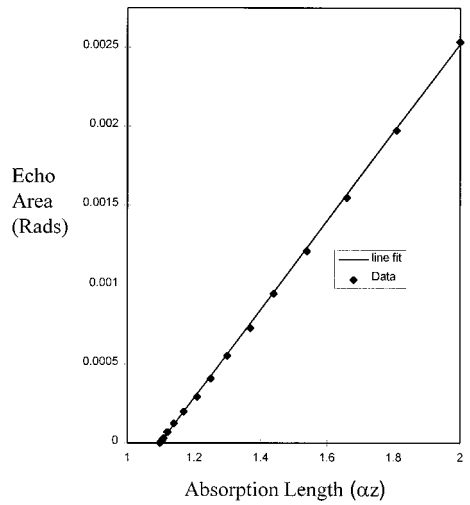

FIG. 3. Two-pulse photon echo maximum area points for brief pulse areas ranging from 0.002π to 0.7π. The points closely match a linear fit for brief pulse areas that range over three orders of magnitude.

of the brief pulse is increased, but reaches this maximum at a larger absorption length. Note that these maximum points all lie roughly on a line as long as the area of the brief pulse is less than approximately 0.7π. We have found an analytic solution for this ''line'' from Eq. (15). For weak data pulses, M_1 is small, and thus Eq. (15) can be expanded in powers of M_1. Keeping the linear term in M_1, one obtains

$$A_e(z)=2M_1M_2^2\,\frac{X-X^3}{1+M_2^2X^2}. \tag{16}$$

To find $A_{e,\max}$ we differentiate Eq. (16) with respect to X and set the result equal to zero. We solve the resulting equation for M_2, substitute the result back into Eq. (16), and obtain

$$A_{e,\max}(z)=\tan\left(\frac{A_{10}}{2}\right)\left[\exp\left(\frac{\alpha z}{2}\right)-3\exp\left(-\frac{\alpha z}{2}\right)\right]. \tag{17}$$

Equation (17) is zero at $\alpha z=\ln(3)$, and thus can be expanded around the $\alpha z=\ln(3)$ point (the optimal absorption length as predicted by the linear theory [15,17]), and keeping the first two leading nonzero terms, the efficiency can be written as

$$\eta_{2\mathrm{PE}}=\frac{A_{e,\max}(\alpha z)}{A_{10}}\cong\frac{\sqrt{3}}{2}\,[\alpha z-\ln(3)]+\frac{\sqrt{3}}{48}\,[\alpha z-\ln(3)]^3. \tag{18}$$

The effect of the third-order term is small.

In Fig. 3 we have plotted the linear term of Eq. (17) and the points from the numerical simulations at which the echo reaches its maximum area for brief pulses ranging from 0.002π to 0.7π. We found that the linear fit accurately predicts the maximum echo area for brief pulses ranging over 3 orders of magnitude. It is also clear from Eq. (17) that $A_{e,\max}$ intercepts the αz axis at ln(3). Thus our theory is in agreement with the linear theory for nonsaturated absorbers in which the maximum efficiency is obtained when the absorption length is equal to ln(3) [17].

Figure 4 illustrates the efficiency of the photon echo process for brief pulse areas ranging from 0.1π to 0.9π. The

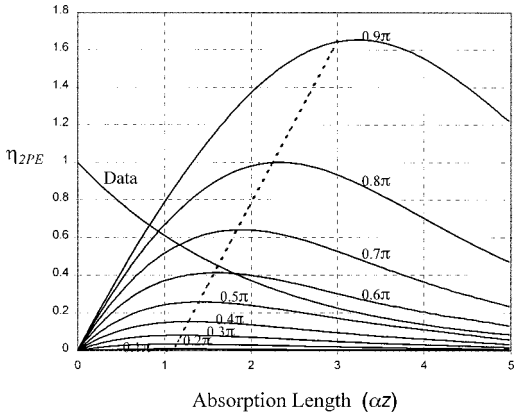

FIG. 4. Two-pulse photon echo efficiency for values of brief pulse areas varying from 0.1π to 0.9π. The relative amplitude of the data pulse and the linear fit to the maximum points (dashed) are also shown.

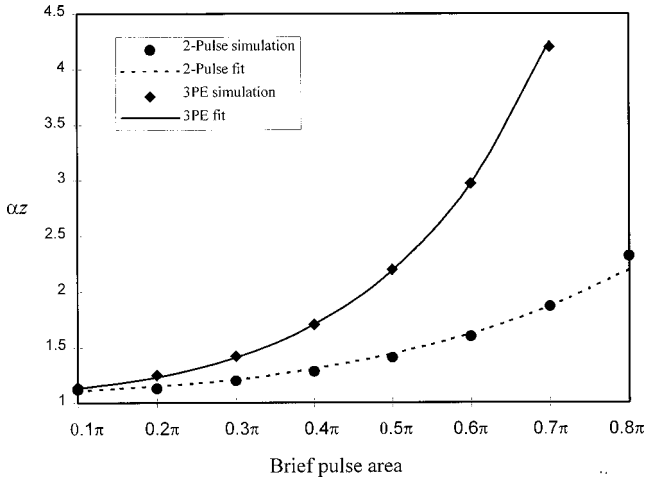

FIG. 5. Absorption length at which the echo signal efficiency becomes maximum as a function of brief pulse area for two-pulse and stimulated echoes. The points are simulation results and the lines are plots of fitting expressions.

efficiency can be defined as the maximum amplitude of an arbitrary point of the echo pulse, $A_{e,\max}$, divided by the amplitude of the corresponding point in the data pulse at the input plane, A_{10}, provided the output is an undistorted replica of the input data. We have chosen this point to be the peak of the last subpulse in the data and echo. The linear dependence of the maximum echo efficiency, $\eta_{2\mathrm{PE}}$, on absorption length for various brief pulse areas is obvious from Fig. 4.

From the plots of Fig. 4 it can be seen that the efficiency predicted by the linear term of Eq. (18) holds very well for brief pulse areas up to approximately 0.7π. At the same time, the output data wave forms shown in Fig. 1 reveal that the output signal shape is almost without distortion (the subpulses are completely separate) for brief pulse areas up to 0.7π, and starts to deform for larger brief pulse areas. Thus, it is observed from the numerical simulations that as long as the output echo signal is almost free from propagation distortions, it obeys Eq. (18) with predicted two-pulse photon echo efficiencies up to 60%.

The exact analytic expression for the absorption length at which the maximum echo efficiency, $(\alpha z)_{\max}$, is obtained for a given brief pulse area is

$$(\alpha z)_{\max}=\ln\left[\frac{1}{2}\left[(M_2^4+10M_2^2+9)^{1/2}+M_2^2+3\right]\right]. \quad (19)$$

Equation (19) is complicated, but a fairly good approximation to it is

$$(\alpha z)_{\max}=\ln(3)\exp(\beta A_{20}^2), \quad (20)$$

where β is a fitting parameter that for the case of the 2-pulse echo is approximately equal to 0.11. Equation (20) approximates Eq. (19) with an error of less than 2% for pulse areas up to 0.6π. Figure 5 shows both a plot of this expression for β equal to 0.11 and the actual values from numerical simulations.

Substitution of Eq. (20) into Eq. (18) results in an expression for the maximum efficiency of the two-pulse echo signal for a given value of brief pulse area

$$\eta_{2\mathrm{PE}}=\frac{\sqrt{3}}{2}\ln(3)[\exp(\beta A_{20}^2)-1], \quad \beta\cong 0.11, \quad A_{20}\leqslant 0.8\pi. \quad (21)$$

This expression holds provided there are no distortions in the output. Therefore, based on the previous discussion regarding distortion, A_{20} has to be less than approximately 0.8π for this expression to be valid. It is interesting to note that the efficiency for $A_{20}=0.8\pi$ is about unity, that is, the maximum output echo signal is about the same size as the input data pulse.

VI. STIMULATED PHOTON ECHO SIMULATION RESULTS

Here we consider the case of a brief ''write'' pulse followed by a data pulse, which causes the information to be stored in the population between the two atomic levels. A third brief ''read'' pulse then causes the information stored in the population to change to a coherence between the two states and to rephase at a time that to first order is equal to the time interval between the first two pulses [18]. The sample then reemits a replica of the data pulse [1]. The stimulated echo does not depend on a coherent phase delay of the absorbers in the two-pulse echo process. In fact, the third pulse can theoretically come at an infinite time after the second pulse. This allows for very long storage times compared to the brief storage time (on the order of microseconds) for the two-pulse echo. In our simulations of the stimulated echo, r_1 and r_2 are set to zero just before the third pulse is applied. This assures that all the information stored in the form of coherences is removed before the application of the third brief pulse, thus simulating the conditions in a physical system after decay of the coherences has occurred. The predicted stimulated echo is now only a result of the information stored in the population gratings. In this study we assume that the areas of the two brief pulses are equal. However, we may find in future studies that the efficiency of the recall process may be enhanced by independently vary-

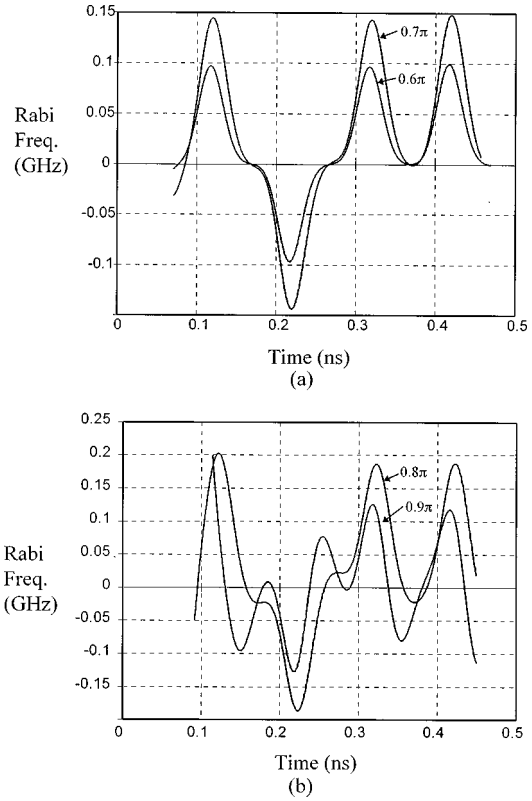

FIG. 6. Stimulated photon echo output signal, for brief pulses of (a) 0.6π and 0.7π, (b) 0.8π and 0.9π.

ing the areas of the brief pulses or perhaps by using frequency chirped pulses.

Unlike the case of the two-pulse echo, the area theorem may not be used directly in the case of the stimulated echo. The reason is that A_e in Eq. (15) refers to the total area of all the pulses that come after the first two pulses. In a stimulated echo, this total area might include the echoes of other pulse combinations as well as the stimulated echo in which we are interested. Moreover, the area theorem is based on the assumption of no coherence loss, whereas the stimulated echo is based on the storage of information as population differences between the two atomic levels, and is not affected by a coherence loss after the second pulse.

The simulation results of the stimulated echo are shown in Figs. 6 and 7. In Fig. 6 the actual shape of the stimulated echo (at the αz where the echo is maximum) for values of brief pulses ranging from 0.6π to 0.9π is shown. Figure 7 illustrates the efficiency of the stimulated echo versus αz for the same data pulse as before and brief pulses ranging from 0.1π to 0.9π. The temporal shape of the echo is nearly distortion free for the 0.6π and 0.7π brief pulses, but signs of distortion can clearly be seen for the case of 0.8π brief pulses, and for 0.9π brief pulses the output is completely distorted. However, if we examine the efficiency plots in Fig. 7, we see that the maximum efficiency for a 0.7π pulse is nearly 150%. Thus two vital criteria for data recall are simultaneously achieved—high echo efficiency and minimal wave form distortion.

If we examine Fig. 7 more closely, it is apparent that, like the 2-pulse echo, the echo efficiency becomes maximum at a larger αz for larger values of brief pulse areas. Moreover, as long as the areas of the brief pulses are each less than about

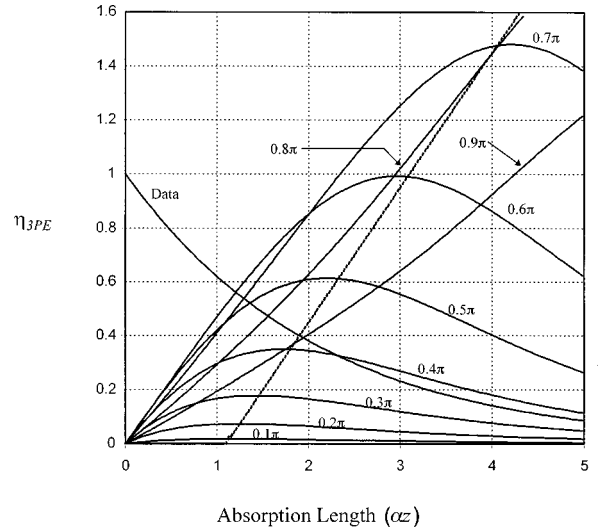

FIG. 7. Stimulated photon echo efficiency for values of brief pulse areas varying from 0.1π to 0.9π. The relative amplitude of the data pulse (when preceded by a 0.1π brief pulse) and the linear fit to the maximum points (dashed) are also shown.

0.7π, the maximum points lie closely on a line that intersects the αz axis at $\alpha z = \ln(3)$. When the brief pulses are 0.8π each, the echo does not have a local maximum within the simulation length, and when they are 0.9π each, the growth of the echo with αz starts to drop.

As with the case of the two-pulse echo, we observe that for the stimulated echo the maximum efficiency points lie closely on a line, but with a slope of 1/2. We now postulate that

$$\eta_{3\mathrm{PE}} = \frac{A_{e,\max}(\alpha z)}{A_{\mathrm{data}}} = \frac{1}{2}\,[\alpha z - \ln(3)], \tag{22}$$

where $A_{e,\max}$ is the maximum amplitude of an arbitrary point in the stimulated echo and A_{data} is the amplitude of the corresponding point in the data pulse. Equation (22) approximates the numerical simulations with a root-mean-square error of less than 5%. It can again be observed that to the extent that the stimulated echo obeys Eq. (22), it is almost free from propagation distortions.

The method used in the case of a two-pulse echo to obtain a second equation for the absorption length at which the echo signal becomes maximum cannot be used here because we do not have analytic results for the stimulated echo. However, Eq. (20) is also a fairly accurate interpolation for the stimulated echo, with the parameter β now equal to 0.28. The actual values from the numerical simulations are compared with a plot of Eq. (20) for β equal to 0.28 in Fig. 5. The maximum efficiency of the echo signal is now given by

$$\eta_{3\mathrm{PE}} = \tfrac{1}{2}\,\ln(3)[\exp(\beta A_{20}^2) - 1], \quad \beta \cong 0.28, \quad A_{20} \leqslant 0.7\pi. \tag{23}$$

As before, the validity of this expression is based on the assumption of no distortion, and so A_{20} should be less than approximately 0.7π.

VII. SUMMARY AND CONCLUSION

We have presented the results of numerical simulations of the evolution of two-pulse and stimulated photon echoes as a function of propagation length αz. These simulations are based on the standard Maxwell-Bloch equations and they predict the possibility of achieving high efficiency echo signals with minimal distortion. We also presented expressions [Eqs. (21) and (23)] that predict the size of the maximum attainable echo as a function of the brief pulse area and the data pulse amplitude. The absorption length at which the echo is maximized may also be found from Eq. (20). For the two-pulse echo the accuracy of these results is reaffirmed by the analytic results obtained from the area theorem. For the stimulated echo simulations, we postulate the relationship between the maximum echo efficiency and the absorption length based on an in-depth understanding of the two-pulse echo.

These results are based on rather ideal assumptions. Wave-form recall efficiency is not well understood and therefore it is appropriate to study it first in isolation. One can then proceed with a more rigorous investigation that includes nonideal behavior of practical systems. In practice, the inherent dampings in the system (which were neglected in our ideal version of the Maxwell-Bloch equations) may limit and reduce the efficiency of the process. Furthermore, our results are based on a plane-wave theory. In a real laser beam, the concept of area becomes radius dependent, and the effects of the beam profile on these results have yet to be studied.

In summary, we have shown that efficient recall of temporally structured weak optical pulses can be obtained via the photon-echo process if the absorption length and pulse area of brief pulses are appropriately chosen. Efficiencies greater than 150% were predicted for both the 2-pulse echo and stimulated echo. It should be noted that the efficiency of the intensity is the square of the amplitude, and thus will be greater than 225%. We have also shown that data pulses can be processed and recalled with very high fidelity at brief pulse areas that maximize efficiency. These results, coupled with recent results of echoes in inverted media [12] and in cavities [19], serve as a motive to further study the possibility of obtaining highly efficient coherent transient based memories and processors.

ACKNOWLEDGMENT

We gratefully acknowledge the financial support of the Air Force Office of Scientific Research under Grant Nos. F49620-93-1-0513, F49620-95-1-0468, and F49620-97-1-0259.

[1] T. W. Mossberg, Opt. Lett. **7**, 77 (1982).
[2] T. W. Mossberg, Opt. Lett. **17**, 535 (1992).
[3] H. Lin *et al.*, Opt. Lett. **20**, 1658 (1995).
[4] W. R. Babbitt and J. A. Bell, Appl. Opt. **33**, 1538 (1994).
[5] W. R. Babbitt and T. W. Mossberg, J. Opt. Soc. Am. B **11**, 1948 (1995).
[6] A. Shen *et al.*, Opt. Lett. **21**, 833 (1996).
[7] S. Kroll and P. Tidlund, Appl. Opt. **32**, 7233 (1993).
[8] W. R. Babbitt, Y. S. Bai, and T. W. Mossberg, Proc. SPIE **639**, 240 (1986).
[9] A. Szabo and J. Heber, Phys. Rev. A **29**, 3452 (1984).
[10] V. L. da Silva and Y. Silberberg, Phys. Rev. Lett. **70**, 1097 (1993).
[11] Y. Silberberg *et al.*, IEEE J. Quantum Electron. **28**, 2369 (1992).
[12] M. Azadeh and W. R. Babbitt, Mol. Cryst. Liq. Cryst. **291**, 269 (1996).
[13] L. Mandel and E. Wolf, *Optical Coherences and Quantum Optics* (Cambridge University Press, Cambridge, 1995).
[14] S. L. McCall and E. L. Hahn, Phys. Rev. **183**, 457 (1969).
[15] E. L. Hahn and N. S. Shiren, Phys. Lett. **37A**, 265 (1971).
[16] Y. S. Bai *et al.*, Appl. Phys. Lett. **45**, 714 (1984).
[17] W. R. Babbitt, Ph.D. thesis, Harvard University (1987).
[18] K. D. Merkel, M. Azadeh, and W. R. Babbitt (unpublished).
[19] T. W. Mossberg (unpublished).